TO-98-15-3 (RP-897)

Measuring Adjacent Building Effects on Laboratory Exhaust Stack Design

David J. Wilson, Ph.D., P.E.
Member ASHRAE

Ian Fabris

Mark Y. Ackerman, P.E.
Member ASHRAE

ABSTRACT

Current methods for designing exhaust stack height and exit velocity are based on avoiding contamination of the roof, walls, and nearby ground surface of the building on which the stack is located. Usually, no account is taken of the effect of adjacent buildings that add turbulence and increase dispersion if they are located upwind and may be contaminated themselves if they are downwind of the emitting building. To account for these adjacent building effects, ASHRAE Research Project 897 used water-channel simulation of the atmosphere to evaluate rooftop contamination in more than 1,700 different configurations of adjacent building height, width, spacing, stack location, stack diameter, height, and exit velocity. Exhaust stacks on scale models of flat-roof buildings were tested using fluorescent dye tracer illuminated by thin laser light sheets, with digital video images to measure dilution in the exhaust plume at roof level air intake locations. The results show that high stacks and exit velocities that represent good design on an emitting building can be less effective and are sometimes counter productive in reducing contamination of the roof of a nearby adjacent building. The implications of the study for developing practical stack design guidelines are discussed in this paper.

INTRODUCTION

Many exhaust stacks from laboratory fume hoods and industrial exhausts are not actually designed but instead are simply specified to have the minimum height, typically about 7 ft (2.1 m), that will meet local fire and building code requirements. For stacks that are designed by making exhaust-to-intake dilution calculations, the effect of adjacent buildings in changing the rate of plume dispersion and deflecting plume trajectories is only accounted for by rough approximations. For example, the current ASHRAE design method in chapter 15 of the *1997 ASHRAE Handbook—Fundamentals* (ASHRAE 1997) specifies that no credit for stack height should be given when the plume passes over a downwind building or rooftop obstacle that is higher than the stack. Denying credit for stack height below obstacles is based on wind tunnel experiments by Wilson and Winkel (1982).

Studies of the effect of buildings on plume dispersion have focused primarily on the added turbulence and flow downwash that affect ground level concentrations from a stack located downwind of the building. Wind tunnel measurements by Robins and Castro (1977a, 1977b), Huber (1989, 1991), Huber and Snyder (1982), Huber et al. (1991), and Thompson (1993) all focused on the effect of a single isolated upwind building affecting a ground-based stack. The effect of the plume from an isolated upwind stack impinging at roof level on a downwind building was investigated in a wind tunnel study by Wilson and Netterville (1978). None of the existing studies dealt with the important question of how a closely-spaced adjacent building will influence the exhaust gas dispersion from a roof-mounted stack on another building.

OBJECTIVES

ASHRAE RP-897 carried out a systematic study of sixteen adjacent and emitting building configurations to determine how adjacent buildings should be accounted for in laboratory stack design. The research project had four distinct objectives:

1. To use scale models of emitting and adjacent building pairs to catalogue the effect of adjacent buildings over a wide range of stack heights, exhaust velocity to windspeed ratios, stack locations, and emitting/adjacent building configurations.

David J. Wilson is a professor, **Ian Fabris** is a graduate student, and **Mark Y. Ackerman** is a faculty service officer, Department of Mechanical Engineering, University of Alberta, Edmonton, Canada.

2. To use the results of this catalogue of building dilution measurements to recommend stack design procedures that improve plume dispersion (and reduce intake contamination) when an adjacent building is present.
3. To compare measured dilutions with dispersion calculations using the computer models ISC3 and SCREEN3 developed by the Environmental Protection Agency (EPA 1995a, 1995b) and the ASHRAE dilution model from chapter 15 of the *1997 ASHRAE Handbook—Fundamentals*.
4. To prepare a commentary on the suitability of existing models for predicting exhaust-to-intake dilution in the presence of adjacent buildings and to evaluate the suitability of availability of design standards such as *ANSI/AIHA Standard Z9.9-1992*, which states that re-entry of fume-hood exhaust should be avoided at nearby buildings as well as on the emitting building.

In this paper, only the first two objectives will be addressed: to describe the experimental measurements of dilution and to recommend methods for improving stack designs that account for adjacent building effects. The detailed discussion of the performance of EPA and ASHRAE dispersion models is presented in the final report of RP-897 (Wilson et al. 1998).

The experiments of Wilson and Winkel (1982) suggest that there may be no benefit from higher stacks when the emitting building roof is enveloped by the flow recirculating zone behind an adjacent upwind building. When the adjacent building is downwind, the plume from a high stack ejected at high exhaust velocity (to avoid contaminating the emitting building roof) may rise and impinge directly on the roof level intakes if the adjacent building is higher than the emitting building. The measurements reported here show that both these undesirable situations do occur and cause large increases in contamination of roof level intakes.

BUILDING AND STACK CONFIGURATIONS

The building configurations used in the study are shown in Figure 1, where they are presented in six different subcategories. The two factors used for categorizing adjacent building effects are (1) whether the upwind or downwind building is emitting the exhaust and (2) the relative roof heights of the two buildings. Figure 1 shows the definitions of step-across, step-up, and step-down roof levels.

All the data shown here is for the single-width buildings (2.5 H wide). Normalized dilution plots for the double-width buildings show the same general trends as the single width buildings and are presented in the final report of the project (Wilson et al. 1998).

For each of the building configurations, 54 combinations of stack location, stack height, and exhaust velocity were tested.

- Three stack locations: 0.25 H from upwind and downwind roof edges and in the center of the roof.
- Three stack heights of $h_s = 0.175$ H, $h_s = 0.25$ H, and $h_s = 0.5$ H to simulate stack heights of 7 ft, 10 ft, and 20 ft on a nominal emitting building with height H = 40 ft.
- Six values of exhaust velocity ratio $M = W_e/U_H$ of 1.0, 1.5, 2.0, 3.0, 5.0, and 8.0, with equal exhaust and ambient air densities $\rho_e = \rho_a$, to produce a non-buoyant momentum jet from the uncapped stack.

These measurements were made using stacks with inside diameter $d = 0.10$ in. (2.54 mm). This $d/H = 0.05$ stack simulated a nominal diameter of $d = 2$ ft (0.61 m) for building height of $H = 40$ ft (12.2 m) in the nominal 240:1 scale. For the sixteen configurations in Figure 1, 1728 combinations were measured for roof level concentrations. To confirm that the results from the $d = 0.05$ H stack could be applied to other stack diameters using appropriate scaling factors, a series of 21 tests were performed to repeat selected configurations using a stack diameter of $d = 0.025$ H, half the size of the standard stack.

Model buildings were constructed by machining solid blocks of aluminum to emitting building height $H = 2.0$ in. (50.8 mm) and equal widths and lengths of 5.0 in. (101.6 mm). Several auxiliary blocks were constructed so that groups of blocks could be arranged to create the 1.5 H and 2.0 H high and 5.0 H wide double-width buildings. One of the single-width blocks was hollowed out, and friction-fit adjustable height stacks were installed in a 0.25 in. (6.35 mm) thick roof. Flexible plastic tubes connected each stack to a manifold valve and a bank of five rotameters to cover the flow needed for the M = 1.0 to 8.0 range.

Surface concentrations for plumes impinging on building walls were also investigated using model buildings with glass roofs and walls with mirrors mounted internally at 45° angles to allow the downward looking video camera to see through the glass roof and out the glass building wall. One of the laser light sheets shown in Figure 1 was realigned to a vertical orientation just in front of the building wall, and plume impingement concentrations were recorded. These wall impingement measurements produced another 972 combinations. The results for these building wall impingement studies are not reported here but may be found in the final project report (Wilson et al. 1998).

SCALE MODEL SIMULATION OF ATMOSPHERIC DISPERSION

Both wind tunnels and water channels can be adapted to produce simulated atmospheric turbulence for dispersion experiments. With both available, the present study chose to use water-channel simulation because of its superior ability to produce full-field video images of plume cross sections using thin laser light sheets to illuminate the entire roof of scale model buildings. Simulating the stack exhaust gas with water allowed us to accurately mix known concentrations of fluorescent dye tracer to produce the exhaust concentration C_e in the water-channel experiments.

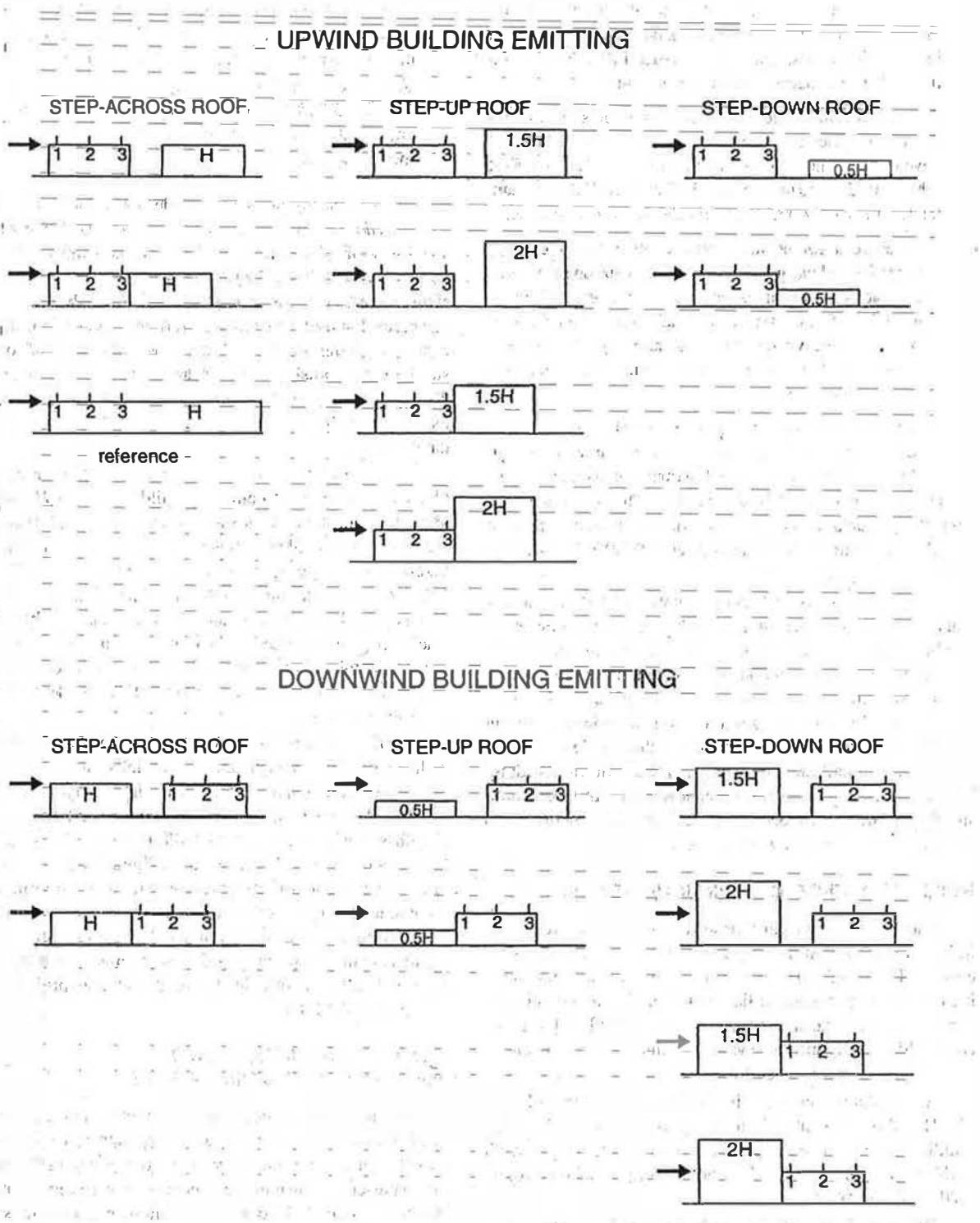

Figure 1 *Adjacent building configurations test in water channel simulation. Building widths of 2.5 H and 5.0 H tested for all 16 configurations.*

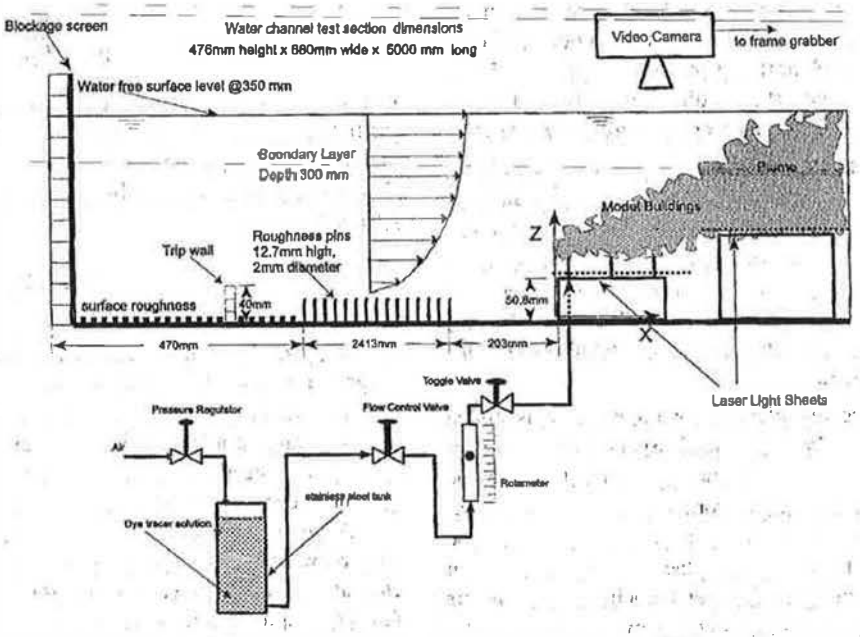

Figure 2 *Water channel flow processing for simulation of atmospheric wind profile and turbulence approaching buildings.*

Simulation of atmospheric diffusion from stacks near buildings requires the following factors to be considered:

- Correct simulation of atmospheric turbulence intensity and eddy scales in the simulated approach wind profile.
- Correct flow reattachment and wake recirculating regions for the model buildings.
- Correct similarity of exhaust gas momentum, buoyancy, velocity profiles, and turbulence in the emerging flow from the laboratory stack.
- Correct scaling of wind-tunnel or water-channel concentration data to an appropriate full-scale atmospheric averaging time. This averaging time is the time during which the plume is allowed to meander back and forth to produce the time-averaged receptor concentration.

Boundary Layer Simulation

The water channel in Figure 2 was specifically designed to model atmospheric dispersion. The 16 ft (4.9 m) long test section allows development of the large eddy structures typical of the lower 300 ft (100 m) of a neutrally stable atmospheric boundary layer. Flow processing to achieve this simulation began with a flow-blockage screen with variable area openings on the downstream side of the flow straightener at the water-channel entrance. This blockage screen helped to rapidly develop a wind boundary layer profile by changing the inlet velocity profile from one that was uniform with height to a closer approximation of the increasing speed with height in the developed boundary layer. After passing over a low wall to generate cross-stream vortices, the flow developed naturally over a plate covered with uniformly distributed nylon pins that were designed to produce an urban roughness boundary layer with a log-law roughness scaling length in $U \propto \ln(z/z_o)$ of z_o=1.60 mm in the water channel, equivalent to a full-scale roughness length of z_o = 380 mm in the 240:1 scale at which the experiments were conducted. The mean velocity profile in Figure 3 was fit with the power law $U \propto z^{0.26}$, typical

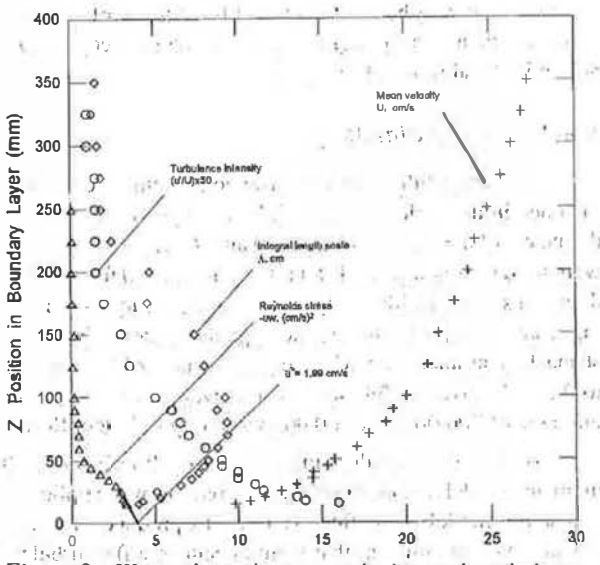

Figure 3 *Water-channel mean velocity and turbulence profiles with no building present. Model scale emitting building height. H = 50.8 mm (2.0 in.) in approximate 240:1 scale.*

of a low-rise urban area (Irwin 1979). In the absence of building models, the water-channel speed at model building height, $H = 2.0$ in. (50.8 mm), was maintained at $U_H = 0.57$ ft/s (174 mm/s). At this speed, the building Reynolds number was $Re_H = U_H H/\nu = 7700$ for a water temperature of 59°F (15°C).

In his review of building flow simulations, Snyder (1993) performed experiments that supported the Reynolds number scaling recommendations of Robins and Castro (1977a). For a turbulent boundary layer wind profile approaching a model building, they found that a correct flow simulation was obtained for Reynolds numbers $Re_H > 3000$ to 4000. Our experiments were carried out at a Reynolds number twice this minimum requirement.

One widely accepted reference for atmospheric dispersion simulation is Snyder (1981), updated in Snyder (1993). Snyder recommends that for correct turbulence intensity and scale simulation, the Reynolds number formed using the surface friction velocity u_* and log-law roughness length scale z_o should be $u_* z_o/\nu > 2.5$. Using the measured value $u_* = 19.9$ mm/s, from the single-component laser doppler velocity measurements shown in Figure 2, our friction velocity Reynolds number was 23, a factor of 10 larger than the required minimum.

Flow Reynolds numbers in the water-channel boundary layer are several thousand times smaller than their full-scale atmospheric counterparts. These low Reynolds numbers in the laboratory flow require that the roughness elements used in the water channel be much larger and more densely packed than would be found in a full-scale atmospheric flow. In order to allow the boundary layer to forget this exaggerated roughness height, a smooth surface the length of 4.0 H was placed in front of the model buildings, as shown in Figure 1. Measurements were made at roof height to confirm that this short readjustment length had a negligible effect on wind speed at roof height in the absence of buildings.

Stack Exhaust Simulation

The correct full-scale stack Reynolds number cannot be matched in the scale model. Stainless-steel tubes with inside diameters of $d = 0.05$ in. (1.27 mm) and $d = 0.1$ in. (2.54 mm) were used to simulate the 1.0 ft (305 mm) and 2.0 ft (610 mm) diameter stacks in 240:1 scale. For exhaust velocity ratios ranging from $W_e/U_H = 1.0$ to 8.0, the large diameter 0.1 in. model stacks had laminar flow, with Reynolds number $W_d\, d/\nu = 400$ to 3200. Equivalent full-scale stacks would have Reynolds numbers of 200,000 to 1,600,000 with fully turbulent flow.

No attempt was made to induce turbulent flow in the small diameter model stacks. Instead, a correction was applied to adjust the model scale flow velocity to produce the same exhaust momentum flux that would occur in a flat turbulent flow profile emerging from a full-scale exhaust stack. A momentum flux correction factor, $\alpha = 2.0$, for laminar flow was used when calculating M, the density-weighted exhaust velocity W_e to windspeed U_H ratio:

$$M = {}^{0.5}\left(\frac{\rho_e}{\rho_a}\right)^{0.5} \frac{W_e}{U_H} \qquad (1)$$

where ρ_e and ρ_a are the exhaust and atmospheric densities. For the flat (uniform) velocity profile that would be expected for highly turbulent flow in full scale, $\alpha = 1.0$. All values of M shown in the figures are full-scale equivalent values calculated using

$$M = 1.414 \frac{W_{e,\,model}}{U_{H,\,model}}, \qquad (2)$$

where ρ_e and ρ_a for the water were used to simulate both atmospheric air and exhaust gas in the model.

To determine the effect of laminar exhaust flow on plume trajectory and turbulent mixing, a series of experiments were carried out using a larger scale stack of 0.35 in. (8.8 mm) ejecting fluorescent dye into the laser light sheet. These tests, with a stack Reynolds number of 1600, showed that the emerging jet underwent a rapid tr nsition to turbulence within ten diameters after exiting with velocity ratios ranging from $M = 1.0$ to 4.0. When a turbulence generator was inserted in this larger model stack to produce a flat turbulent exit profile, the entrainment and mixing into the bent-over jet was indistinguishable from its laminar counterpart at the same momentum-adjusted velocity ratio M after the plume had traveled ten diameters from the stack tip. These experiments confirmed that momentum-adjusted laminar exhaust flows in the model stacks provide an accurate simulation of jet mixing, plume rise, and dispersion.

Plume Spread Simulation

The final step in assessing the accuracy of scale model simulation was to measure crosswind plume spread in the absence of buildings to determine the appropriate concentration averaging time that was being simulated in the water channel. This full-scale concentration averaging time cannot be determined by using a scale factor to adjust the concentration sampling time used to collect water-channel data. In the water channel, the glass sidewalls prevent the l rge crosswind plume meandering that occurs for averaging times longer than several minutes in the atmosphere.

The effective averaging time for the water channel was determined by measuring crosswind plume spread σ_y in the water channel using 100 second averages of 1000 frames of digital plume images of fluorescent dye illuminated by laser light sheets. A streamlined isokinetic injector tube 0.135 in. (3.45 mm) inside diameter ejected dye tracer parallel to the flow at building height $z = H = 2.0$ in. (50.8 mm) above the surface with no building models present. Figure 4 shows measured plume spread over the range of downwind distances z/H where building models would be tested. The data shows that an effective initial source size σ_o adds linearly to the turbulence induced spread:

$$\sigma_y = A_y x' + \sigma_o \qquad (3)$$

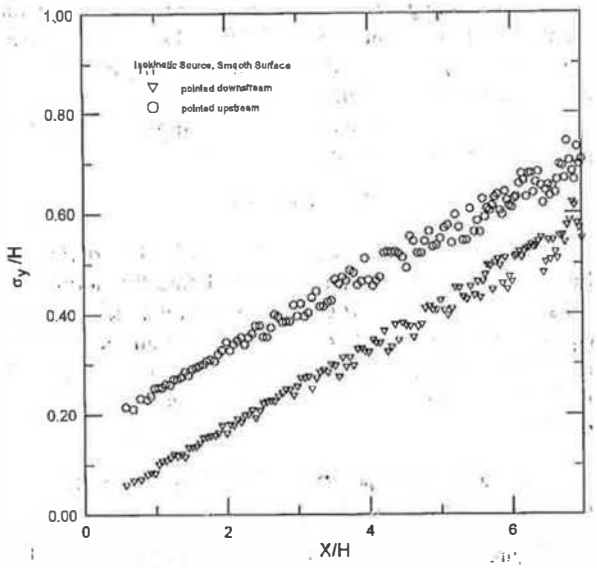

Figure 4 *Crosswind plume spread of σ_y/H with no buildings for plumes from an isokinetic fluorescent dye tracer source injected at height H and location x = 0 where the emitting building will be positioned.*

Here, x' is the distance $x' = (x - x_{stack})$ from the stack, with the origin $x = 0$ at the point where the upwind wall of the emitting building is located (see Figure 2). In the absence of buildings, we found $A_{y,model} = 0.080 \pm 0.04$ averaged over several different tests.

Full-scale urban dispersion measurements of McElroy and Pooler (1968) were used by Briggs to develop 60-minute averaging time plume spread equations for σ_y and σ_z for EPA models ISC3 and SCREEN3. For the neutrally stable case simulated here, these functions are linear in the first 1500 ft (≈ 500 m) from the source, with $A_{y,atmos} = 0.16$ for 60-minute averages in the neutrally stable atmosphere (class D) simulated in the water channel (EPA 1995a). Using the widely-accepted 0.2 power law to adjust A_y values for changes in averaging time t_{avg},

$$\frac{A_{y,model}}{A_{y,atmos}} \approx \left(\frac{t_{avg,model}}{t_{avg,atmos}}\right)^{0.2} \quad (4)$$

For $A_{y,model} = 0.08$, $A_{y,atmos} = 0.16$, and $t_{avg,atmos} = 60$ min, we calculated from Equation 4 that $t_{avg,model} = 1.9$ min. Using this indirect method, we were able to interpret our water channel measurements as representing two-minute averages in the full-scale atmosphere.

Finally, it is worth noting that the linear relation of Figure 3 between plume spread and downwind distance allows the building model experiments to be scaled up or scaled down as long as the size of the two buildings together does not exceed the range of about 500 m where the linear spread function is valid. This means that the scale model buildings with length $L = 2.5$ H can be used to represent building heights a factor of 4 higher and lower, ranging from about $H = 10$ ft (3.05 m) to $H = 160$ ft (48.8 m) rather than the single nominal building size of $H = 40$ ft (12.2m) chosen for the research project.

In the following discussion, we will refer to an $H = 40$ ft building height with stack heights $h_s = 7$ ft, 10 ft, and 20 ft above the roof. These nominal values will help us visualize a typical full-scale situation, but in fact may be scaled up and down by about a factor of four to represent other buildings with the same stack to building height ratios h_s/H.

DILUTION MEASUREMENTS WITH FLUORESCENT DYE TRACER

Rooftop concentration measurements were made using disodium fluorescein dye as a tracer in the water injected from the stacks, as shown in Figure 2. The dye was illuminated by laser light sheets generated by a 4 W argon ion laser and recorded using a video camera looking down through the surface of the water at the building rooftops. Digital images of the plume were obtained using a 10-bit (1024 step) frame grabber board to directly average 1000 frames acquired at 10 frames per second over a 100 second sampling time.

The single beam from the 4 W argon ion laser was split into two beams that were carried by fiber-optic cables to the water channel where they were processed through converging and cylindrical lenses to produce a thin light sheet about 0.04 in. (1.0 mm) thick diverging at about a 10° angle over the building rooftops. The building models and surrounding ground surface plates were painted flat black to minimize reflections.

A black and white CCD video camera with a 3:1 zoom lens was used to record video images of the plume. Because the camera looked through the water surface (see Figure 2), a plastic float that spanned the width of the water channel was anchored upstream to remove surface ripples over the building models. The camera lens was fitted with a yellow filter to remove the blue-green laser light reflections and allow only the green-yellow dye fluorescence to be recorded.

Video Image Calibration

Each of the 480 by 640 pixels in the frame grabber array were individually calibrated by placing an open-bottomed box over the models and filling it with concentrations of fluorescent dye solution. Digital images over the model roofs then gave individual pixel calibration values of concentration vs. intensity counts on the frame grabber. By including the model buildings, direct compensation was obtained for surface reflections. The three stacks on the emitting building roof passed through the laser sheet and cast shadows and produced bright reflections. These shadows were too dark to be corrected by the direct calibration technique and are visible in dilution contour plots (Figure 5). The dilution data points near the stacks were obscured by reflections and are removed from the graphs (Figure 8).

Calibration of the camera and frame grabber produced a linear intensity-concentration response over a 250:1 range of concentrations in the calibration box. This linear response allowed us to use real-time averaging of the pixel intensities for the 1000-frame sample, followed by conversion of the average intensity to average concentration.

The corners of the emitting building provided a scale reference to convert pixels into position distances on the average video image. The width and length of each pixel element was about 0.02 in. (0.5 mm or 0.01 H) on the model roof. This high spatial resolution was found to be unnecessary, and only every fifth pixel was recorded in the final data arrays. This resulted in each of the single width building rooftops (2.5 H long and wide) having a dilution measurement array of 50 × 50 points on the roof surface giving 2500 measurements on each building roof to define contours of constant concentration and profiles of minimum dilution.

NORMALIZED DILUTION FUNCTIONS

The dilution factor D is defined as the ratio of exhaust to receptor concentration, $D = C_e/C$, where C is the pollutant concentration at any receptor and C_e is the pollutant concentration in the exhaust gas. This dilution depends on the volume flow rate from the stack and the ability of the atmosphere to disperse pollution, characterized by variables such as windspeed and vertical and crosswind plume spreads. In order to present the results of our measurements in a form that can be used for stack design, we normalized these measured dilutions in a form that allows them to be adjusted to a variety of full-scale atmospheric wind conditions and varying ratios of exhaust velocity to windspeed. The appropriate normalizing factor was derived by considering roof level concentration for the Gaussian concentration profile for a plume dispersing in homogeneous turbulence over a roof with the plume reflected from the impervious roof surface (Panofsky and Dutton 1984).

$$C_{roof} = \frac{C_e Q_e}{\pi U_c \sigma_y \sigma_z} \exp\left(\frac{-(h_s + \Delta h)^2}{2\sigma_z^2}\right), \qquad (5)$$

where C_{roof} is the roof level concentration on plume centerline, U_c is the effective wind velocity for plume convection, and C_e is the concentration of pollutant (in the same units ppm or $\mu g/m^3$ as C_{roof}) in the total exhaust volume flow rate Q_e. The plume spreads σ_y and σ_z in the crosswind and vertical directions vary with distance x' from the stack. The stack height is h_s with a final plume rise Δh above the top of the stack.

The minimum (i.e., plume centerline) dilution is defined as $D_{min} = C_e/C_{roof}$. Rearranging Equation 5 to define the normalized dilution,

$$\frac{D_{min} Q_e}{U_H H^2} = \pi \left(\frac{U_c}{U_H}\right) \frac{\sigma_y}{H} \frac{\sigma_z}{H} \exp\left(\frac{\left(\frac{h_s}{H} + \frac{\Delta h}{H}\right)^2}{2\left(\frac{\sigma_z}{H}\right)^2}\right), \qquad (6)$$

where the building height H has been used to normalize the dilution to be consistent with normalizing distance as x/H. The wind speed U_H is observed at emitting building height $z = H$ above ground with no buildings present.

For a non-buoyant momentum jet, Briggs (1975, 1984) gives the final momentum rise height as

$$\Delta h = 3.0\ Md, \qquad (7)$$

where the density-weighted velocity ratio M is defined in Equation 1. We used Equation 7 to define the normalized exhaust velocity ratio Md/d_{ref} with the reference diameter equal to the stack tested, $d_{ref} = 0.05$ H. For all the measurements shown in this paper, $d = d_{ref}$ and the normalized exhaust velocity to windspeed velocity ratio was equal to the actual ratio M.

DILUTION FOR UPWIND EMITTING BUILDING STEP-ACROSS ROOFS

Figure 5 shows dilution contours for a flat-roof building at a low exhaust velocity $M = 1$ and a higher exhaust velocity of $M = 3$, both for the medium (0.25 H) stack height, equivalent to $h_s = 10$ ft on an $H = 40$ ft high building. At the low exhaust velocity, the plume is downwashed into the roof recirculation region at the leading edge of the building and

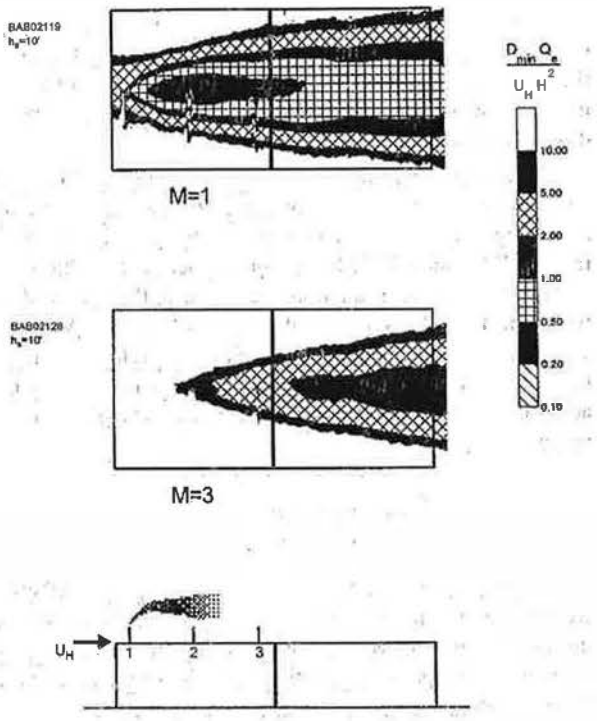

Figure 5 Dilution contours on the flat-roof building (step-across roof, no gap) for the medium 10 ft stack height (h_s/H = 0.25) with exhaust velocity to windspeed ratios of M = *1 an* M = *3.*

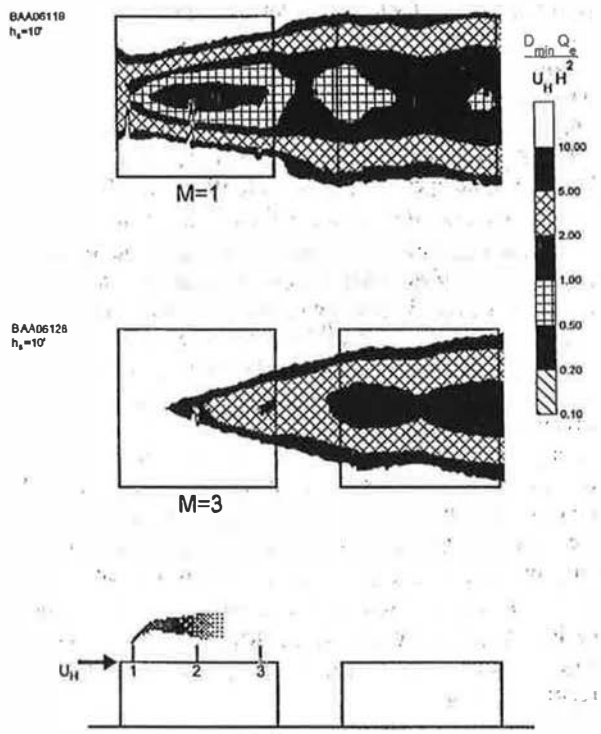

Figure 6 *Dilution contours for step-across roof with 1.0 H gap between buildings for the medium 10 ft stack height (h_s/H = 0.25) with exhaust velocity to windspeed ratios of* M = *1 and* M = *3.*

produces significant concentrations upwind to the roof edge. Note the distortion in the dilution contours caused by light sheet shadows from the three stacks.

Figure 6 shows the same stack height as Figure 5 but with a gap of 1.0 H between the buildings. Along the plume centerline, the dilution increases in the gap but then decreases as material trapped in the gap is sucked up over the roof of the downwind adjacent building.

Figure 7 presents the normalized minimum dilution on the plume centerline to show the effect of gap width between the buildings. The data points in Figure 7a for M = 1.0 and 3.0 are the same as shown in Figure 6.

Reference Building Dilution Measurements

In all the normalized dilution plots, we have included lines showing the normalized dilution measured on the long flat-roofed reference building (Figure 1). Measurements from this building give a baseline with which to compare adjacent building effects at each exhaust velocity ratio. Although measurements were made for six velocity ratios, for clarity we have shown only three.

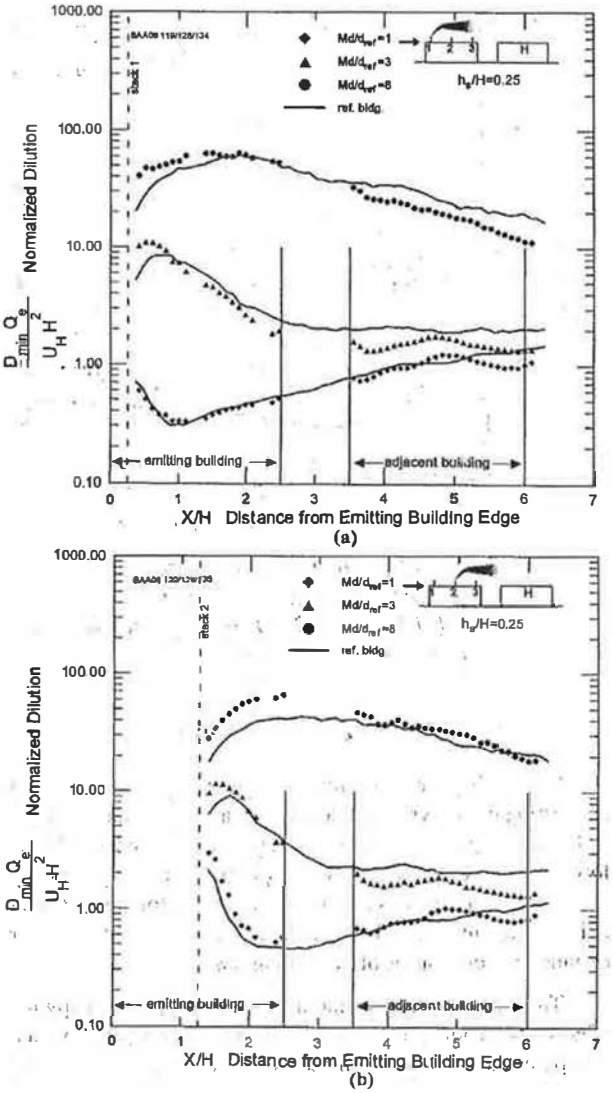

Figure 7 *Effect of gap between buildings (symbols) and no gap (solid lines) references with step-across roof for medium 10 ft stack height (h_s/H = 0.25) on the upwind emitting building.*

Effect of Gap Between Buildings for Step-Across Roof

Comparing Figure 7a and 7b with the reference building data, we see that the gap between the buildings has a negligible effect on dilution for step-across roof levels. Differences between the lines and the data symbols can be attributed to the ±30% run-to-run random variability between centerline concentrations from the 1000-frame averages. Because we are plotting normalized dilution, this run-to-run repeatability includes uncertainties in water channel speed U_H and in the exhaust flow, Q_e, along with the uncertainties inherent in quantitative video imaging.

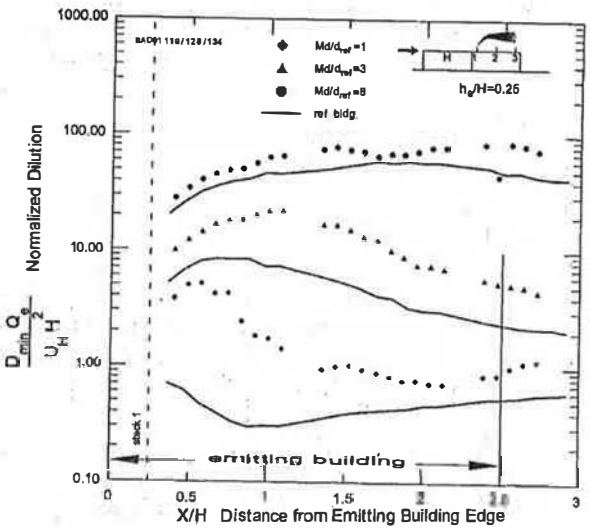

Figure 8 *Effect of locating a stack far from upwind roof edge. Solid lines for reference building are for stack 1 located 0.25 H from upwind roof edge (see Figure 1).*

Stack Location: Central vs. Upwind Edge

Comparing the measured dilution in Figure 7, we see an interesting effect when the stack is located near the roof edge in Figure 7a vs. the central stack shown in Figure 7b. At the lowest exhaust velocity ratio $M = 1.0$, the near-edge stack has dilution 2 to 5 times less than the central stack for the first stack heights downwind. This effect disappears at the higher exhaust velocity ratios of $M = 3.0$ and 8.0.

The adverse effect of mounting a stack near the upwind edge of the roof is even more apparent in Figure 8, which compares the stack location near the upwind edge of the reference building roof with data taken on a downwind emitting building with no gap, placing the stack at $x = 2.75$ H from the upwind edge of the roof. For the reference building, stack 1 is only $x = 0.25$ H from the upwind roof edge (Figure 1). An important point for designers to note is that the measured dilution in Figure 8 from the edge-mounted stack on the reference building (solid lines) is a factor of 2 to 10 less than for the same stack located far from the upwind roof edge (data points).

Using the flow visualization measurements of Wilson (1979), the *1997 ASHRAE Handbook—Fundamentals,* chapter 15, Equation 23 gives the height of the roof edge recirculation cavity as $H_c = 0.22\,H^{0.67}Y^{0.33}$, where Y is the crosswind width of the building. For the single building widths reported here, $Y = 2.5$ H and the height of the roof edge recirculation cavity was $H_c = 0.30$ H. The top of the stack with $h_s = 0.25$ H in Figure 2.8 ended inside this edge recirculation cavity, and rooftop dilution factors were considerably reduced. This dramatically illustrates the disadvantage of locating a stack in the region of high wind velocity caused by the flow accelerating over the roof edge near a zone of flow recirculation.

These observations lead to a clear recommendation to designers: avoid locating stacks near the edge of the roof where high windspeed can deflect the plume into the roof edge recirculating cavity.

STEP-UP ROOF LEVEL WITH EMITTING BUILDING UPWIND

Figure 9 shows the plume from a low level stack on an upwind building impinging on the wall of a higher downwind adjacent building with its step-up roof level. From Figure 9, it is easy to imagine that the worst case for contaminating the downwind building roof would be a high exhaust velocity that carries the plume trajectory to the level of the downwind roof. At the other extreme, a plume with very low exhaust velocity would remain close to the roof level of the emitting building and be swept around the sides of the adjacent building with

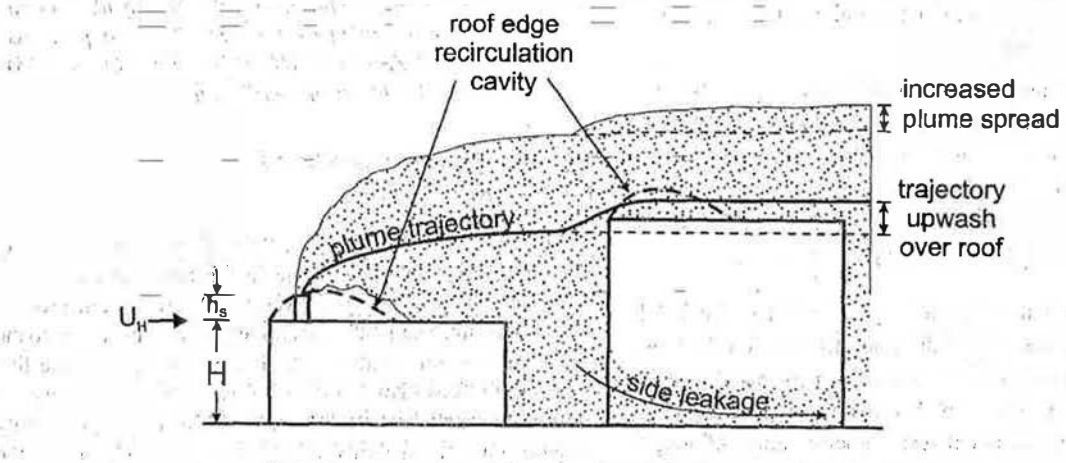

Figure 9 *Plume trajectory and spread from an upwind emitting building over a downwind adjacent building with a step-up roof.*

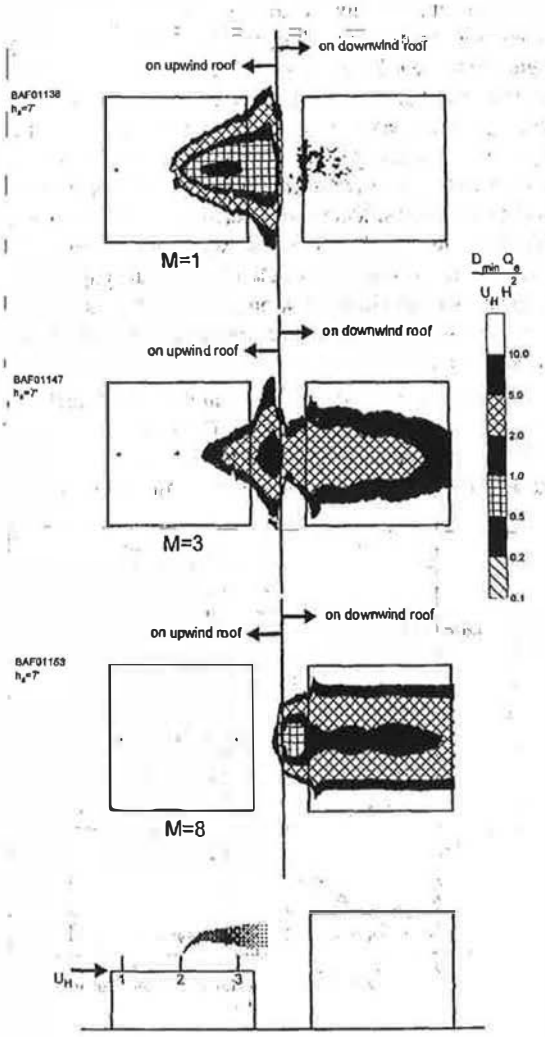

Figure 10 *Dilution contours on step-up roof 2H adjacent building for a short 7 ft stack height* (h_s/H = 0.175) *with exhaust velocity to windspeed ratios of* M = *1,* M = *3, and* M = *8.*

only a small fraction being carried over the roof. This situation would minimize adjacent building roof contamination at the expense of contaminating the roof of the emitting building.

The dilution contours in Figure 10 clearly show the difficulty faced by stack designers with high adjacent downwind buildings. At low exhaust velocity $M = 1.0$, the exhaust plume from the central stack produces very low dilution (high concentration) areas on the emitting building, but passes around the sides of the adjacent building leaving its roof uncontaminated. At a moderate exhaust velocity ratio, M = 3.0, about the same level of contamination occurs on the emitting and adjacent building roofs. At the highest exhaust velocity, $M = 8.0$, the momentum jet causes the plume to rise high above the emitting building to heavily contaminate the roof of the adjacent building. At $M = 8.0$, the high concentration (low dilution) plume core is easily visible as it is carried over the edge of the adjacent building roof. The effect of the diverging streamlines in the decelerating flow approaching the high adjacent building is readily apparent in the broadening of the plume dilution contours as they approach the adjacent building.

Figures 11a and 11b show the combined effect of stack height and exhaust velocity in producing worst-case dilutions on the adjacent rooftop. To test our hypothesis that the worst-case condition occurs when the centerline of the undisturbed plume trajectory is at the height of the adjacent roof, use the final momentum jet rise from Equation 7 to calculate the point

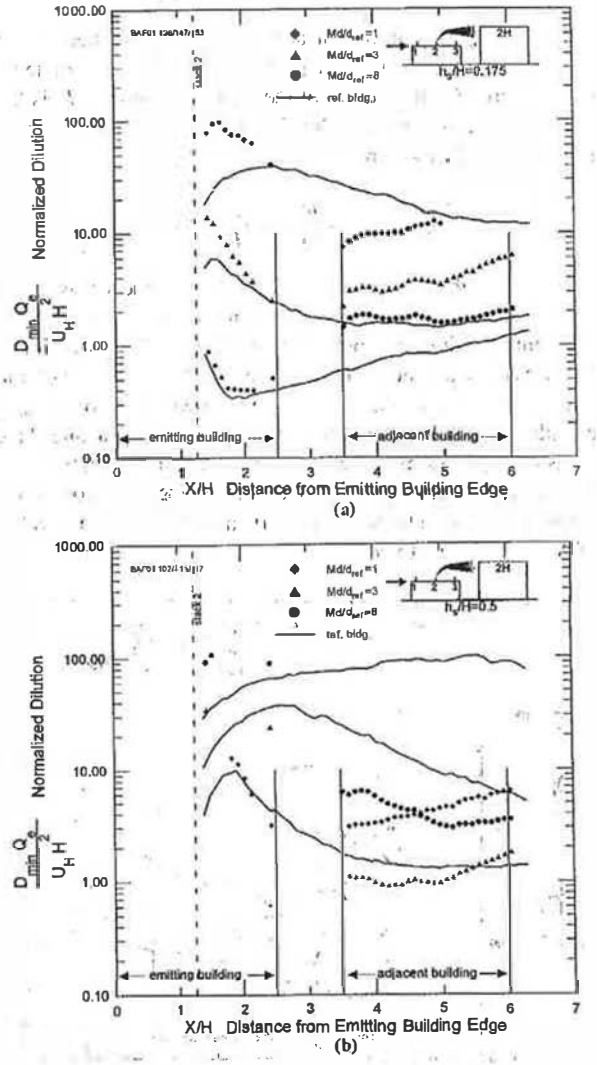

Figure 11 *Effect of stack height on minimum dilution for a step-up roof on a 2 H adjacent building with 1.0 H gap for short 7 ft* (h_s/H = 0.175) *and tall 20 ft* (h_s/H = 0.5) *center stacks on the upwind emitting building.*

TABLE 1
Calculated Impact Heights for Plumes Striking a 2H Adjacent Building

M	Figure 11a h_s/H = 0.175	Figure 11b h_s/H = 0.5
	$\Delta z_{impact}/H$ Equation 9	$\Delta z_{impact}/H$ Equation 9
1.0	−0.68	−0.35
3.0	−0.38	−0.05 Observed Worst Case
8.0	+0.38 Observed Worst Case	+0.70

impact for the plume trajectory on the downwind adjacent building as

$$\Delta z_{impact} = (H + h_s + 3Md) - H_{adj}, \quad (8)$$

where Δz_{impact} is the height at which an undisturbed plume will pass above the roof of an adjacent building roof level H_{adj}, where H is the height of the emitting building, h_s is the stack height, and $3Md$ is the final momentum jet rise from Equation 7. If we normalize by H,

$$\frac{\Delta z_{impact}}{H} = 1 + \frac{h_s}{H} + 3M\frac{d}{H} - \frac{H_{adj}}{H}. \quad (9)$$

The height Δz_{impact} will be negative if the undisturbed plume trajectory, shown as a dashed line in Figure 9, strikes the adjacent building wall below the roof. Note that Equation 9 includes no adjustment for the upward deflection of the plume trajectory, shown in Figure 9. Table 1 shows values of Δz_{impact} calculated for the configurations in Figures 11a and 11b. Considering the simple assumptions inherent in Equation 9, it does a remarkably good job of predicting the worst-case exhaust velocity ratio for both short and tall stacks as the value of Δz_{impact} closest to zero.

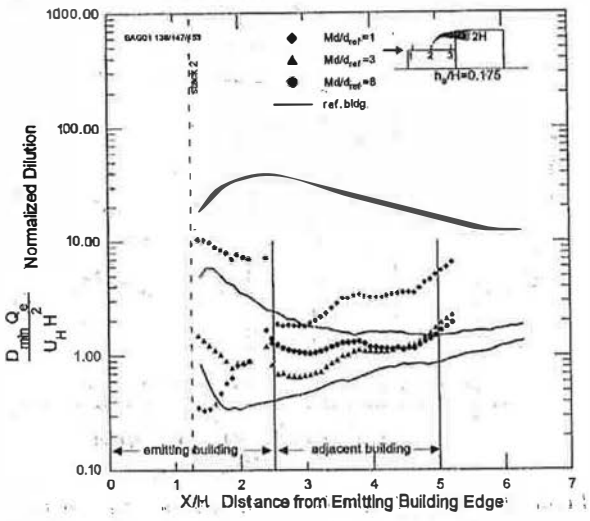

Figure 12 Effect of gap between buildings (compare with Figure 11b) on minimum dilution for a step-up roof on a 2 H adjacent building with a short center 7 ft stack (h_s/H = 0.175) on the upwind emitting building.

The higher downwind adjacent building affects the dilution on the emitting building roof in unpredictable ways. In Figure 11a, the dilution close to the stack is a factor of 2 to 4 times larger than the reference building case at high exhaust velocity with a gap between the emitting and adjacent buildings. In contrast, comparing Figure 12 to Figure 11a shows that when the gap between the buildings is closed, the dilution on the emitting building roof becomes a factor of 5, smaller than the reference building case when the exhaust velocity ratio is high. This reversal of effects when the gap is removed suggests that there is still a strong need for case-specific studies using wind tunnel and water-channel scale models for critical situations.

When there is a gap between buildings, the location of the stack does not appear to be critical. Figure 13 shows the effect of stacks located at the upwind and downwind edge of the emitting building. Both produce about the same normalized

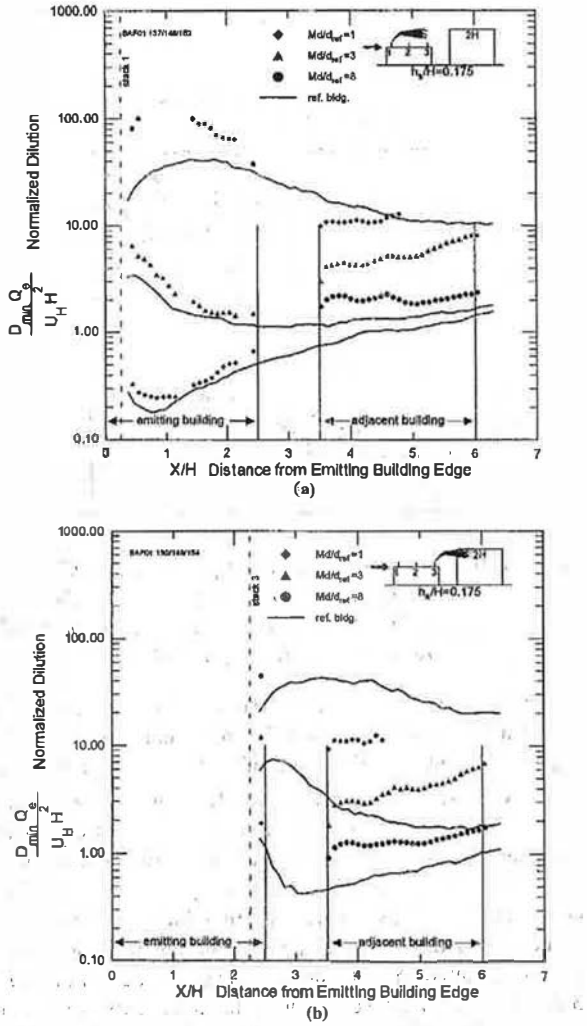

Figure 13 Effect of stack location 1 vs. 3 (upwind edge vs. downwind edge) on minimum dilution for a step-up roof on a 2 H adjacent building with 1.0 H gap and a short 7 ft (h_s/H = 0.175) stack on the upwind emitting building.

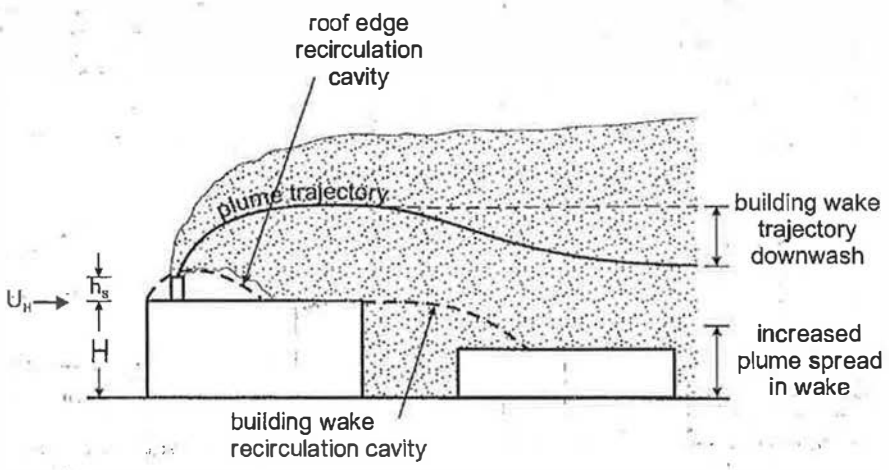

Figure 14 Plume trajectory and spread from an upwind emitting building over a downwind adjacent building with a step-down roof.

dilution on the roof of the adjacent building, and there is only a modest increase in dilution over the emitting building roof caused by the presence of the adjacent building.

EMITTING BUILDING UPWIND WITH STEP-DOWN ADJACENT ROOF

The effect of a step-down building located downwind from the emitting building is shown in Figure 14. The dilution contours in Figure 15 indicate that the plume continues to spread in a relatively normal fashion even though it has been entrained by the wake recirculation behind the emitting building. Measurements of crosswind plume spread σ_y on the downwind building roof were compared to measured spreads over the reference building and found to differ by no more than a few percent. This surprising result suggests that the effects of a step-down roof can be expressed of in terms of increased vertical plume spread σ_z combined with a step-down in the location of the roof receptor.

Figure 16 shows that the net effect for a step-down building is that the dilution is always greater on its roof than for an equivalent reference building with a flat roof. In addition, Figure 16 shows that there is virtually no effect of having a gap between the upwind emitting building and the downwind step-down adjacent building. These same results occurred for the other stack heights and exhaust velocities tested.

As a general rule-of-thumb, ignoring the step-down roof with an upwind emitting building will result in a conservative design that underestimates actual dilution by factors of 2 to 5 on the step-down roof.

DOWNWIND EMITTING BUILDING WITH STEP-UP ROOF FROM LOWER ADJACENT BUILDING

Figure 17 shows schematically the effect of an upwind building that adds turbulence and helps deflect streamlines before they arrive at the emitting building. This makes the

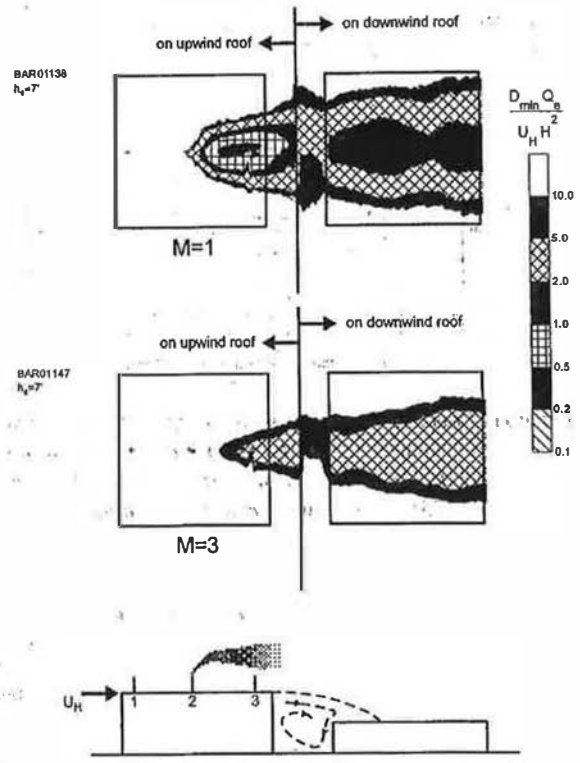

Figure 15 Dilution contours for step-down roof level 0.5 H adjacent building with a short 7 ft central stack height (h_s/H = 0.175) with exhaust velocity to windspeed ratios of M = *1 and* M = *3.*

downwind building look shorter and reduces the size of its roof edge recirculation cavity.

Figure 18 shows that the effect of a lower upwind adjacent building is always helpful, producing significant increases in dilution compared to the flat roof reference building. This was

BACK TO PAGE ONE

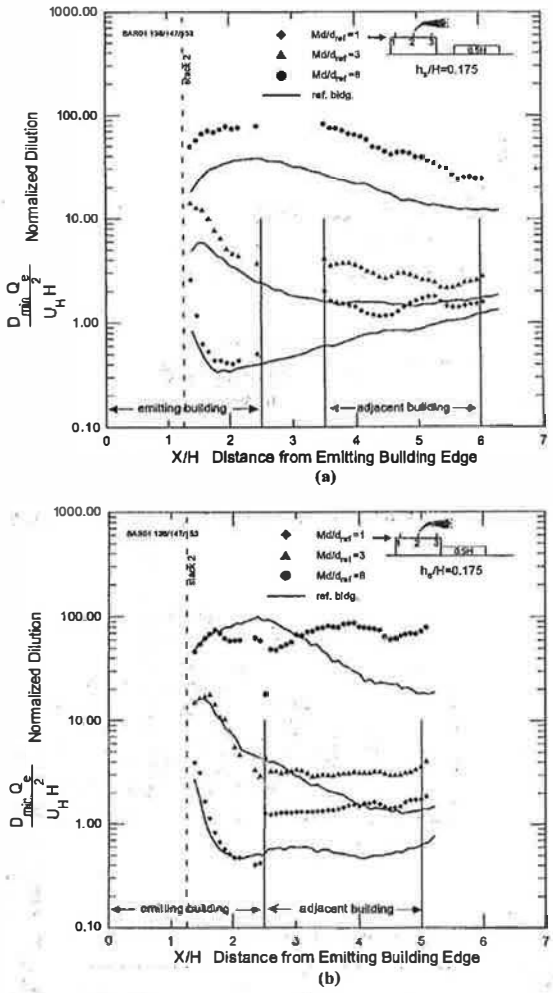

Figure 16 Effect gap between buildings on minimum dilution for a step-down 0.5 H adjacent building with a short 7 ft center stack height (h_s/H = 0.175) on the upwind emitting building.

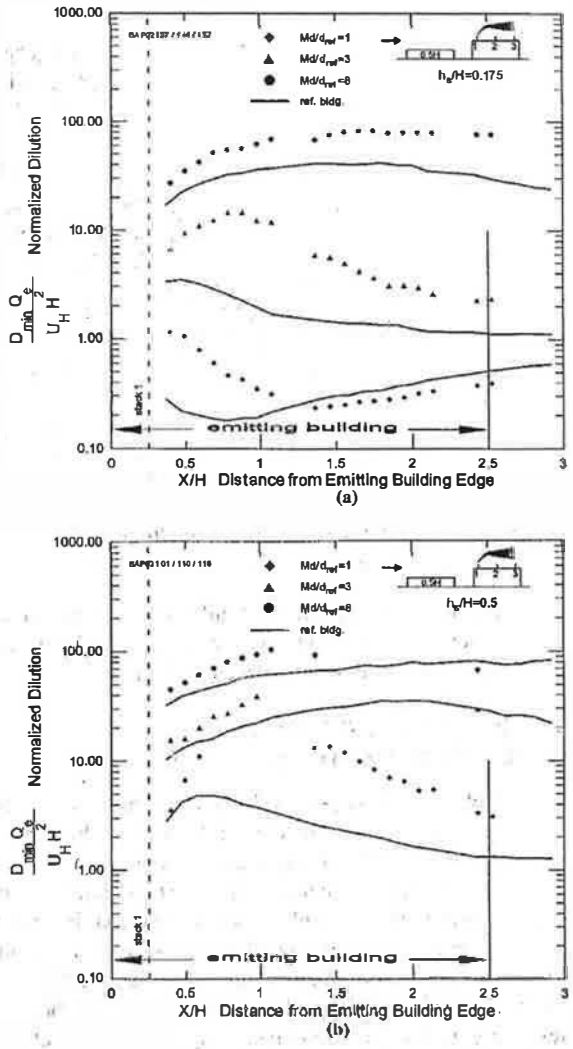

Figure 18 Effect of stack height on minimum dilution for a step-up roof with short 7 ft (h_s/H = 0.175) and tall 20 ft (h_s/H = 0.50) edge stacks on the downwind emitting building.

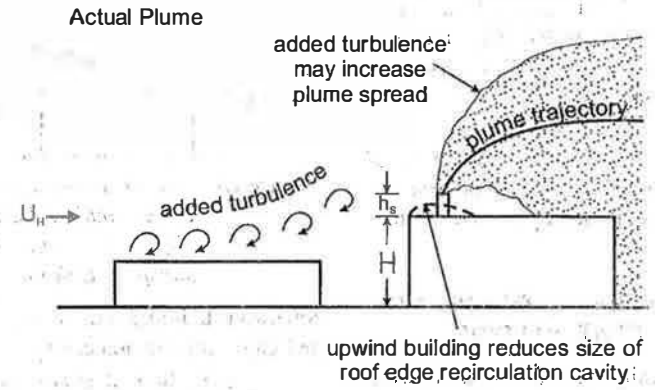

Figure 17 Plume trajectory and spread over an emitting building with a step-up roof located downwind from the adjacent building.

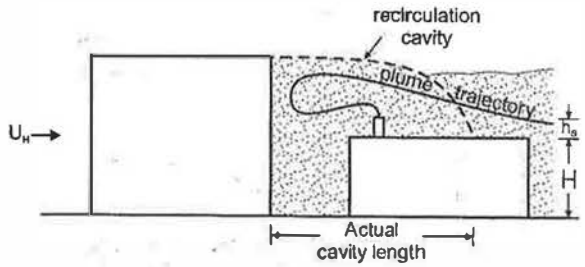

Figure 19 Plume trajectory and spread of exhaust from a central stack on a step-down roof. The exhaust is trapped in the flow recirculation cavity.

true even for the high stack in Figure 18b that extended well above the roof edge recirculation cavity.

STEP-DOWN EMITTING BUILDING WITH HIGHER UPWIND ADJACENT BUILDING

Figure 19 shows the trapping and recirculation of the exhaust gas plume from a short stack on a step-down downwind emitting building. The conventional model of these trapped plumes is that they fill the entire crosswind and vertical wake behind the building with a relatively uniform concentration. The dilution contours in Figure 20 provide a surprising contradiction to this conventional view. At the low exhaust velocity ratio M=1.0, the plume from the short stack is trapped

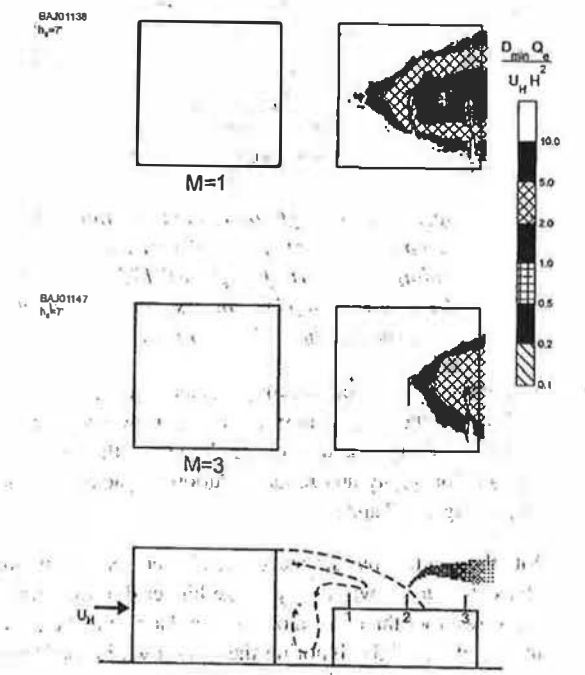

Figure 20 Dilution contours from a short 7 ft (h_s/H = 0.175) stack on a step-down roof. At an exhaust velocity to windspeed ration M = 1 the plume is trapped in the recirculation cavity and carried upwind from the central stack. At M = 3, the exhaust jet escapes cavity recirculation.

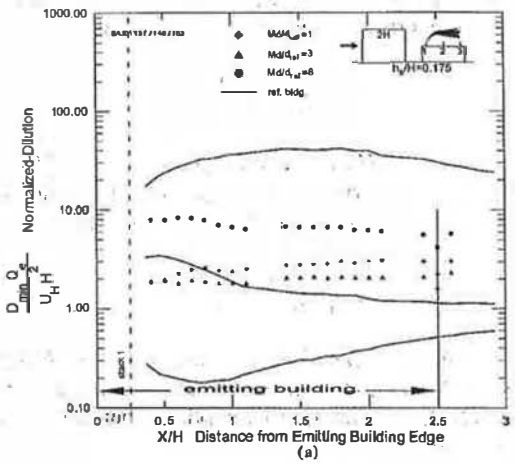

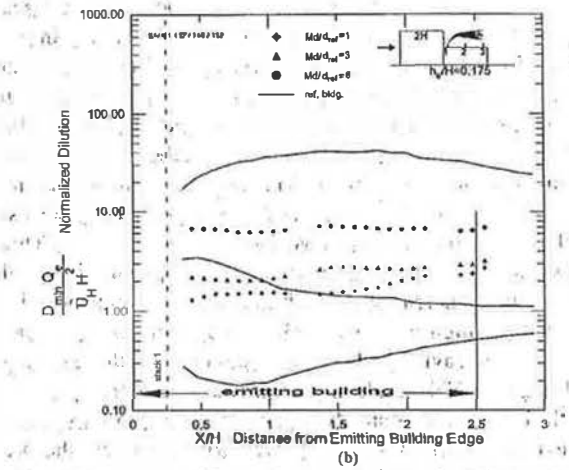

Figure 21 Effect of 1.0 H gap between buildings on minimum dilution from a short 7 ft (h_s/H = 0.175) edge stack on the emitting building located downwind from the 2 H adjacent building.

and carried upwind from its central stack location. However, the dilution contours do not fill the crosswind wake uniformly and the plume behaves more like a point source plume with its virtual origin shifted upwind. At M=3.0, the exhaust jet is strong enough to penetrate the cavity, and although the plume is rapidly dispersed to roof level, none of it appears upwind of the stack location. Figure 21 shows that there is virtually no effect on dilution of removing the gap between the two buildings if exhaust is trapped in the recirculation region for both cases.

The major advantage of increasing exhaust velocity is to provide initial dilution by jet entrainment. The initial dilution D_o caused by an entrainment into a bent-over momentum jet was derived by Wilson and Lamb (1994) and is used in the *1997 ASHRAE Handbook—Fundamentals*, chapter 15, Equation 17. Here we adapt it for use in a recirculation cavity by

using an effective windspeed, U_s, in the cavity rather than the undisturbed approach-flow windspeed U_H, to write

$$D_o = 1 + 13.0\frac{W_e}{U_s}. \qquad (10)$$

Because $U_s < U_H$ in the recirculation cavity, $W_e/U_s > 1$, and the initial "1" term can be neglected in almost all cases, and, for two different exhaust velocities W_{e1} and W_{e2}, we have

$$\frac{D_{o1}}{D_{o2}} \approx \frac{W_{e1}}{W_{e2}} = \frac{M_1}{M_2}. \qquad (11)$$

With this approximation, we expect the $M = 8.0$ data to have about 8 times the dilution of the $M = 1.0$ data in Figures 21a and 21b. The actual measured ratio is about a factor of 6 close to the stack.

Figures 22a and 22b show how stack position and stack height affect the fraction of the plume that is trapped in the cavity. The measured concentrations upwind of the central stack location show that part of the plume remains trapped in the recirculation cavity even for the high stack h_s/H=0.5 at the highest exhaust velocity M=8.0. However, there is a factor of 100 increase in roof level dilution using the high stack at the high exhaust velocity (see Figure 22b) compared to the lowest stack at the slowest exhaust velocity (see Figure 22a). This result suggests that the factor of 8 expected increase in initial dilution from increasing the exhaust velocity is enhanced by allowing the high stack to have 90% of its exhaust escape the recirculation cavity and avoid contaminating the emitting building roof. This result emphasizes the need for designers to use the highest stacks and the highest exhaust velocities possible to reduce roof level contamination even for stacks that are trapped within recirculation cavities from high upwind buildings.

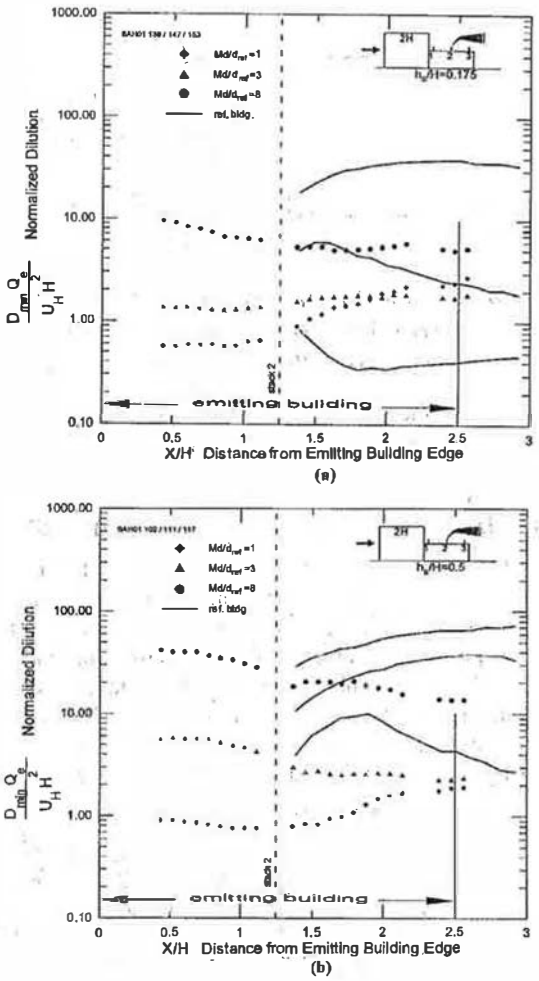

Figure 22 Effect of stack height on minimum dilution from a step-down roof to a downwind emitting building with short 7 ft (h_s/H = 0.175) and tall 20 ft (h_s/H = 0.5) stacks. Plumes from both stacks are trapped in the recirculation cavity.

CONCLUSIONS AND DESIGN GUIDELINES

Measurements of normalized exhaust dilution on emitting and adjacent building rooftops are consistent with common-sense deductions from flow patterns and recirculation zones that can be sketched around the pairs of buildings. The effect of adjacent buildings on dilution can be easily seen by direct comparison with measurements on an equivalent flat roofed long reference building.

The gap between an emitting and adjacent building had a negligible effect on dilution except for the case of an upwind emitting building with a higher downwind adjacent building. In this case, the downwind adjacent building blocks the flow over the emitting building roof and can dramatically decrease the roof level dilution on the upwind emitting building.

Guidelines for Stack Designers

In spite of the fact that plume trajectories and turbulent dispersion around pairs of emitting and adjacent buildings are extremely complicated, there are some general guidelines to aid designers in avoiding contamination of roof level intakes.

- Designers should avoid locating stacks near the edge of a roof, where the high windspeed in the flow accelerating over the roof edge can deflect the plume into the roof edge recirculation cavity and reduce dilution by factors of 2 to 10. See Figures 7 and 8.

- With the emitting building upwind, a lower step-down roof adjacent building will always have higher dilution on the step-down roof than would occur on a flat roof at the emitting building height. Ignoring the step-down in roof level will produce conservative designs. See Figure 16.

- If the lower adjacent building is upwind of the emitting building, it will block the flow approaching the emitting building, producing lower velocities and recirculation cavities on the emitting building roof and increasing dilution by

BACK TO PAGE ONE

factors of 2 to 10 on the emitting building roof. See Figure 18.

- Designers should use increased exhaust velocity to produce jet dilution when the plume will be trapped in the recirculation cavity from a high upwind adjacent building. This initial dilution is directly proportional to exhaust velocity, and increasing exhaust velocity by a factor of 5 will give an extra factor of 5 in dilution everywhere on the emitting building roof, including regions within the flow recirculation cavity. Using both a high stack and high exhaust velocity in these situations helps the exhaust jet escape from the upwind building recirculation cavity.
- When the adjacent building is higher than the emitting building, designers should try to avoid placing air intakes on the adjacent building at heights above the roof level of the emitting building. Then, use the highest stack and exit velocity possible on the emitting building.

ACKNOWLEDGMENTS

This research was supported by joint funding from ASHRAE RP-897 and a Natural Sciences and Engineering Research Council of Canada Individual Research Grant to DJW.

REFERENCES

ASHRAE. 1997. *1997 ASHRAE handbook—Fundamentals*, Chapter 15. Atlanta: American Society of Heating, Refrigerating and Air-Conditioning Engineers, Inc.

Briggs, G.A. 1975. Plume rise predictions, Chapter 3. Lectures on Air Pollution and Environmental Impact Analyses, American Meteorological Society, Boston, 29 Sept. - 3 Oct, 1975: 59-111.

Briggs, G.A. 1984. Plume rise and buoyancy effects, Chapter 8. Atmospheric Science and Power Production, D. Randerson (ed.) U.S. Dept. of Energy DOE/TIC-27601: 327-366.

Huber, A.H. 1989. The influence of building width and orientation on plume dispersion in the wake of a building. *Atmospheric Environment*, 23: 2019-2116.

EPA. 1995a. User's guide for the industrial source complex (ISC3) dispersion models: Volume 2—Description of model algorithms. U.S. Environmental Protection Agency, Research Triangle Park, North Carolina, document EPA-454/B-95-003b.

EPA. 1995b. SCREEN3 model user's guide. U.S. Environmental Protection Agency, Research Triangle Park, North Carolina, document EPA-454/B-95-004.

Huber, A.H. 1991. Wind tunnel and Gaussian plume modeling of building wake dispersion. *Atmospheric Environment*, 25A:1237-1249.

Huber, A.H., and W.H. Snyder. 1982. Wind tunnel investigation of the effects of a rectangular-shaped building on dispersion of effluents from short adjacent stacks. *Atmospheric Environment*, 16: 2837-2848.

Huber, A.H., S.P. Arya, S.A. Raiala, and J.W. Borek. 1991. Preliminary studies of video images of smoke dispersion in the near wake of a model building. *Atmospheric Environment*, 25A: 1199-1209.

Irwin, J.S. 1979. A theoretical variation of the wind profile power-law exponent as a function of surface roughness and stability. *Atmospheric Environment* 13: 191-194.

McElroy, J.L., and F. Pooler. 1968. The St. Louis dispersion study. US Public Health Services, National Air Pollution Control Administration, Report AP-53.

Panofsky, H.A., and J.A. Dutton. 1984. *Atmospheric turbulence: Models and methods for engineering applications*. New York: John Wiley and Sons. pp. 235-237.

Robins, A.G., and I.P. Castro. 1977a. A wind tunnel investigation of plume dispersion in the vicinity of a surface-mounted cube—Part I: Flow field. *Atmospheric Environment*, 11: 291-298.

Robins, A.G., and I.P. Castro. 1977b. A wind tunnel investigation of plume dispersion in the vicinity of a surface-mounted cube—Part II: The concentration field. *Atmospheric Environment*, 11: 299-311.

Schulman, L.L., and J.S. Scire. 1993. Building downwash screening model for the downwind recirculation cavity. *Journal of the Air and Waste Management Association* 43: 1122-1127.

Snyder, W.H. 1981. Guidelines for fluid modeling of atmospheric diffusion. Environmental Protection Agency, Research Triangle Park, North Carolina, Technical Report EPA-600/8-81-009.

Snyder, W.H. 1993. Some observations on the influencing of stratification on diffusion in building wakes. *Proceedings of the Institute of Mathematics and its Applications, Meeting on Stably Stratified Flows*, Sept. 21-23, University of Surrey, Guildford, England.

Thompson, R.S. 1993. Building amplification factor for sources near building: A wind tunnel study. *Atmospheric Environment*, 27A: 2313-2325.

Wilson, D.J. 1979. Flow patterns over flat roofed buildings and application to exhaust stack design. *ASHRAE Transactions* 85(2): 284-295.

Wilson, D.J., and E.H. Chui. 1987. Effect of turbulence from upwind buildings on exhaust gas dilution. *ASHRAE Transactions* 93(2): 2186-2197.

Wilson, D.J., and B.K. Lamb. 1994. Dispersion of exhaust gases from roof level stacks and vents on a laboratory building. *Atmospheric Environment* 28: 3099-3111.

Wilson, D.J., and D.D.J. Netterville. 1978. Interaction of a roof level plume with a downwind building. *Atmos. Environment* 12: 1051-1059.

Wilson, D.J., and G. Winkel. 1982. The effect of varying exhaust stack height on contaminant concentration at roof level. *ASHRAE Transactions* 88(1): 513-533.

Wilson, D.J., I. Fabris, J. Chen, and M.Y. Ackerman. 1998. Adjacent building effects on laboratory fume hood exhaust stack design. Final Report of ASHRAE RP-897, February.